International Journal of Pharmaceutics 478 (2015) 464–475

Contents lists available at ScienceDirect

International Journal of Pharmaceutics

journal homepage: www.elsevier.com/locate/ijpharm

Structural insight into the physical stability of amorphous Simvastatin dispersed in pHPMA: Enhanced dynamics and local clustering as evidenced by solid-state NMR and Raman spectroscopy

Martina Urbanova, Adriana Sturcova, Jana Kredatusova, Jiri Brus *

Institute of Macromolecular Chemistry, Academy of Sciences of the Czech Republic, Czech Republic

ARTICLE INFO

Article history:
Received 14 October 2014
Received in revised form 4 December 2014
Accepted 5 December 2014
Available online 6 December 2014

Keywords:
Solid dispersions
Simvastatin
Pharmaceuticals
Solid-state NMR
Raman spectroscopy
Fluorescence

ABSTRACT

New drug formulations are sought for poorly water-soluble substances because there is a risk of compromised bioavailability if such substances are administered orally. Such active pharmaceutical ingredients can be reformulated as solid dispersions with suitable water-soluble polymers. In this contribution, formulation of a novel and physically stable dispersion of Simvastatin in poly (2-hydroxypropyl) methacrylamide (pHPMA) is demonstrated. Due to the limited water sorption of pHPMA and a high T_g, the prepared dispersion is more suited for oral administration and storage compared with neat amorphous Simvastatin. Surprisingly, the rate of global reorientation and the internal motion of Simvastatin molecules were enhanced and exhibited dynamical heterogeneities when incorporated into the pHPMA matrix. As revealed by solid-state nuclear magnetic resonance combined with Raman spectroscopy exploiting the fluorescence phenomenon the mobility of the ester and lactone components increased considerably, whereas the naphthalene ring remained rigid. Furthermore, the solid dispersion was found to be nano-heterogeneous with nanometer-sized Simvastatin domains. The presence of these clusters had no impact on the dynamics of the rigid pHPMA chains. Thus, the diffusion of Simvastatin molecules through the glassy pHPMA walls and the subsequent transformation of the clusters into larger crystallites were prevented. No crystallization was detected for more than two years.

1. Introduction

As follows from the US Pharmacopeia (29th ed.), approximately 70% of APIs are solid dosage forms that are administered orally. Unfortunately, some compounds with desirable activity may never realize their potential because the properties of the bulk material display unfavorable bioavailability. Particularly, for poorly water-soluble drugs, which comprise 40% of new chemical entities currently being discovered, oral administration is problematic because it may pose a risk of compromised bioavailability. Thus, pharmaceutical research focuses on increasing the absorbency of these substances. Generally, improving the solubility of these substances is a crucial step for the successful development of new drugs. The formulation of these active pharmaceutical ingredients (APIs) as solid dispersions in a polymer matrix is one of the most promising methods (Al-Obaidi et al., 2011; Brough and Williams, 2013; Chiou and Riegelman, 1971; Sekiguchi and Obi, 1961). In many respects, the resultant multi-component blends are fundamentally more complex than formulations containing crystalline API, and the advanced characterization of such systems is currently an extremely active area of pharmaceutical and academic research (Brus et al., 2011; Policianova et al., 2014; Urbanova et al., 2013).

Simvastatin is a drug that is scarcely soluble in water. It has pleiotropic effects, strengthens bone tissue, and is used for the treatment of hypercholesterolemia and osteoporosis (Garip and Severcan, 2010; Gerber et al., 2004; Parhami et al., 2000). The therapeutic applications of Simvastatin could be widened if new formulations are developed. In addition, the stability of Simvastatin must be improved and better controlled. Three crystal forms (forms I, II and III) of Simvastatin are known. Forms II and III are only stable at low temperatures and are thus inappropriate for patients (Husak et al., 2010). Amorphous Simvastatin has a relatively low T_g of approximately 33 °C, i.e., it is difficult to obtain a stable amorphous product and store it in the powdered form. Because the temperature during storage and handling may rise

* Corresponding author. Tel.: +420 296 809 350; fax: +420 296 809 410
E-mail addresses: urbanova@imc.cas.cz (M. Urbanova), sturcova@imc.cas.cz (A. Sturcova), kredatusova@imc.cas.cz (J. Kredatusova), brus@imc.cas.cz (J. Brus).

http://dx.doi.org/10.1016/j.ijpharm.2014.12.007
0378-5173/

above T_g, there is always a possibility that the final product will be present in a supercooled rubbery state (Ambike et al., 2005; Kothari et al., 2014; Pokharkar et al., 2006).

An alternative to a neat amorphous phase is the reformulation of a drug as solid dispersion in an appropriate water-soluble matrix. Polyvinylpyrrolidone (PVP) and polyethylene glycol (PEG) are the most widely used polymers for the preparation of solid dispersions. In the case of Simvastatin, solid dispersions prepared with either PVP or PEG exhibited the largest improvement in wettability and dissolution rate (Silva et al., 2010). The tablets gradually released Simvastatin with a final quantity greater than 80% in 60 min. However, the solid dispersion of Simvastatin in PVP indicated chemical degradation of the drug. Another danger in the formulation of these systems results from their thermodynamic instability. The amorphous drugs, as well as their solid dispersions, are at high-energy states that are thermodynamically metastable and may undergo a phase transformation into the crystalline phase. Generally, the higher tendency of an amorphous system to crystallize is attributed to the higher molecular and segmental dynamics of the system at a given temperature. In this respect, the safe storage temperature should be at least 50 °C lower than T_g (Hancock et al., 1995; Tian et al., 2014).

Amorphous Simvastatin has recently been demonstrated as an example of a drug whose high mobility does not lower its physical stability (Simoes et al., 2013, 2014). Therefore, evaluating the changes in the molecular dynamics of Simvastatin after its transformation from a neat amorphous state to a solid dispersion is of interest. In this study, we have focused on the preparation and detailed characterization of the structure and dynamics of a new type of solid pharmaceutical dispersion of Simvastatin in poly(2-hydroxypropyl) methacrylamide (pHPMA). Although pHPMA is a biocompatible polymer with a high potential for generating efficient drug delivery systems in solution (Hongrapipat et al., 2008; Kopecek et al., 2001; Rihova et al., 1992; Ulbrich and Subr, 2010), the literature shows surprisingly limited attempts to use pHPMA as a matrix for drug formulations.

In general, pharmaceutical solids are specific systems in which detailed physicochemical and structural characterization is mandatory. However, the application of traditional tools, such as X-ray single crystal or X-ray powder diffraction analysis, is strongly limited for the analysis of multi-component and largely amorphous pharmaceutical products. In addition to differential scanning calorimetry (DSC), which is the most widely used technique for the characterization of amorphous, solid dispersions, there are many established and emerging techniques that have been shown to provide useful information. Among numerous analytical techniques that are applicable to these systems, modern Raman and solid-state nuclear magnetic resonance (NMR) spectroscopy occupy outstanding positions. These techniques are capable of providing complete structural data at molecular and at atomic resolution, respectively.

The present study reports on the evaluation of the mobility and stability of Simvastatin molecules dispersed in a pHPMA polymer matrix and characterizes the structure and interactions between the low-molecular component (API) and the polymer chains. For this study, we used traditional tools, such as wide-angle X-ray spectroscopy (WAXS) and DSC combined with Raman spectroscopy (including analysis of the fluorescence phenomenon) and solid-state NMR (ss-NMR). This approach enabled us to explore the thermodynamic behavior, the possibility of mixing at the molecular level, the internal dynamics of both components, the changes in the free volume and the molecular packing. In this manner, our aim was to obtain a more in-depth understanding of the self-assembly processes involved in the formation of an API dispersion in the excipient. The comprehensive characterization of fundamental material descriptors will ultimately lead to the formulation of more robust solid dispersion products.

2. Materials and methods

2.1. Materials and sample preparation

Solid dispersions were prepared from powdered crystalline Simvastatin (Biocon, India, $C_{25}H_{38}O_5$, M_w = 418.566 g/mol, Scheme 1), pHPMA (poly(2-hydroxypropyl) methacrylamide, synthesized at the Institute of Macromolecular Chemistry, ASCR, M_w = 81,000 g/mol), and ethanol (Lach-Ner Czech Republic). Ethanol solutions of Simvastatin (1.2 wt.%) and pHPMA (2.8 wt.%) were allowed to evaporate freely in a Teflon beaker. The total composition of the prepared solid dispersions was maintained at 70 wt.% of polymer and 30 wt.% of Simvastatin. Any traces of ethanol in the resulting products were removed by vacuum evaporation. The prepared solid dispersions of Simvastatin in pHPMA are labeled as Sim_pHPMA throughout this work. Amorphous Simvastatin was prepared by the melting and quenching–cooling method: Simvastatin was heated to 145 °C for approximately 10 min, and the melt was rapidly cooled to room temperature (Graeser et al., 2008; Simoes et al., 2014).

2.2. Water uptake of the polymer matrices

Finely powdered polymers (PVP, M_w = 360,000 g/mol, Sigma–Aldrich, Czech Republic and pHPMA) were dried at 110 °C in a vacuum oven for 24 h. After drying, the polymers were placed into Petri dishes and left to absorb water at laboratory conditions (25 °C, 70% relative humidity). The absorbed water content was determined by thermogravimetric analysis (TGA) after 15 min, 30 min, 60 min and 7 days of exposure; each experiment was repeated three times. TGA of the samples was performed using a PerkinElmer Pyris 1 thermogravimetric analyzer in the temperature range of 30–300 °C at a rate of 5 °C/min. The sample size in all of the experiments was 4–7 mg, and the flow rate of the nitrogen purge gas was fixed at 30 cm^3/min. The water content was evaluated as the mass loss in the temperature interval from 30 to 150 °C.

2.3. Differential scanning calorimetry

DSC analyses were performed on a PerkinElmer DSC 8500 calorimeter with nitrogen purge gas (20 cm^3/min). The instrument temperature and heat flow were calibrated using indium as a standard. Samples of approximately 10 mg were hermetically sealed in aluminum crucibles, and a single hole was punched in the lid. An empty pan of the same type was used as a reference. Thermograms were recorded at a heating rate of 20 °C/min from −10 to 200 °C. In the case of neat Simvastatin, the measurement

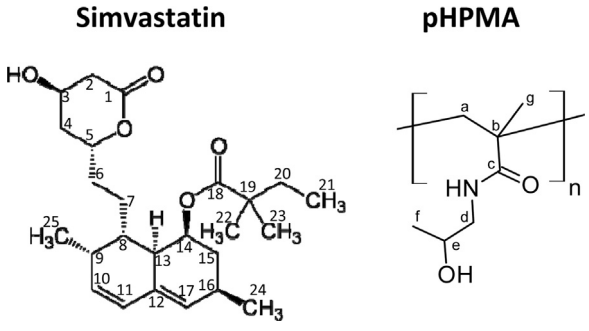

Scheme 1. Chemical structures of the applied components: the active pharmaceutical ingredient (Simvastatin) and the polymer (pHPMA).

was taken only to 160 °C, and the T_g was recorded during the second heating cycle. A preliminary run at 45 °C for 60 min was used for the solid dispersion of Simvastatin in pHPMA. The glass transition temperature was identified as the midpoint between the glassy and rubbery branches of the DSC trace, and the melting temperature was the maximum of the corresponding endotherm plots.

2.4. Raman spectroscopy

Raman spectra on films (solid dispersions and neat amorphous Simvastatin) and on powder samples (neat pHPMA and neat crystalline Simvastatin) were collected on a Renishaw inVia Reflex Raman spectrometer using a HeNe laser with an excitation wavelength of 632.8 nm. A research-grade Leica DM LM microscope with an objective magnification of 50 was used to focus the laser beam onto the sample. The scattered light was analyzed by the spectrograph with a holographic grating of 1800 lines mm^{-1}. A thermo-electric-cooled CCD detector (578 × 385 pixels; the pixel size was 22 μm × 22 μm) registered the dispersed light. Each experiment was performed at the laboratory temperature, and each spectrum consisted of ten accumulations. In the case of the Simvastatin dispersion in pHPMA, 12 spectra were obtained, corresponding to 12 points. The points were randomly chosen from the total area (2.9 mm × 0.5 mm). An average of the 12 spectra was digitally calculated and used for analysis.

2.5. Solid-state NMR spectroscopy

Solid-state NMR spectra were measured at 11.7 T using a Bruker Avance III HD 500 WB NMR spectrometer in 4-mm ZrO_2 rotors. The ^{13}C and ^{15}N cross-polarization (CP) magic angle spinning (MAS) NMR spectra were measured at a spinning frequency of 11 kHz, a $B_1(^{13}C)$ field nutation frequency of 62.5 kHz, a contact time of 1.75 ms, and with a repetition delay of 5 s. The ^{13}C-detected $T_1(^1H)$ relaxation times were measured using a saturation-recovery experiment in which the initial train of ^1H saturation pulses was followed by a variable delay (0.01–15 s). To measure the ^{13}C-detected $T_{1\rho}(^1H)$ relaxation times, an initial $^1H(90^\circ)$ pulse was followed by a variable ^1H spin-lock pulse for 0.1–25 ms. The intensity of the ^1H spin-locking field in frequency units was 80 kHz. $T_1(^{13}C)$ and $T_{1\rho}(^{13}C)$ relaxation experiments were performed at two temperatures (296 and 310 K) with a $B_1(^{13}C)$ spin-locking field intensity corresponding to $\omega_1/2\pi = 62.5$ kHz. Site-specific measurements of one-bond $^1H-^{13}C$ dipolar couplings under Lee–Goldburg conditions (Lee and Goldburg, 1965) were achieved by the "domain-selective" (Brus and Urbanova, 2005) amplitude-modulated (AM) PISEMA experiments (Dvinskikh et al., 2003). 2D $^1H—^{13}C$ FSLG HETCOR NMR experiments were performed using frequency-switched Lee–Goldburg (FSLG) homo decoupling ($\omega_1/2\pi = 100$ kHz), which was applied during the detection period t_1 and consisted of 64 increments of 512 scans each. The CP mixing period was set to 100–1500 μs. Glycine was used as an external standard to calibrate the ^{13}C and ^{15}N NMR chemical shift scales (176.03 and 35.45 ppm, respectively), whereas L-Ala was used to calibrate the ^1H NMR scale (the low-field NH_3 signal at 8.5 ppm and the high-field CH_3 signal at 1.2 ppm). The frictional heating of the spinning samples was mitigated by active cooling, and temperature calibrations (Brus, 2000) were performed with $Pb(NO_3)_2$.

3. Results and discussion

3.1. Water absorption

Although pHPMA is frequently used for drug delivery of therapeutics covalently bound to the polymer chains (Kopecek et al., 2001; Ulbrich and Subr, 2010), the utilization of pHPMA as a polymer matrix for the formulation of solid drug dispersions and subsequent controlled drug release is surprisingly overlooked. To verify the potential of pHPMA for the proposed application and observe its advantages over traditionally used polymers, such as PVP, we first tested the kinetics of water adsorption, which is critical for the chemical stability of hydrolysable drugs dispersed in the polymer matrix.

As clearly demonstrated by the sorption profiles determined under laboratory conditions (Fig. 1), the kinetics of water adsorption was significantly slower in pHPMA compared to PVP. The moisture content of pHPMA increased linearly from 0.4 wt.% at 0 min to 2.6 wt.% at 65 min, whereas the PVP matrix absorbed water exponentially, reaching a maximum value of 8.0 wt.% after the first 30 min. Moreover, pHPMA also exhibited a lower equilibrium moisture content after a seven-day exposure (8.7 wt.%) compared with 13.5 wt.% for PVP. These findings indicate that pHMPA can better protect Simvastatin or other sensitive drugs against chemical decomposition caused by long-term exposure to residual water present in the polymer matrix.

3.2. Differential scanning calorimetry (DSC)

The second critical property of the polymer to be considered as a matrix for the advanced formulation of drugs with low solubility is the capability to molecularly interact with the active compound and to form homogenous systems at the nanometer scale. DSC is among the traditional techniques that are applied to probe the miscibility in multi-component solids via glass transition temperature (T_g) measurements.

As shown in Table 1, the glass transition temperature of the prepared dispersion Sim_pHPMA ($T_{g,Disp} \approx 73$ °C) was between the T_g values of neat amorphous Simvastatin ($T_{g,Sim} \approx 33$ °C) and neat pHPMA ($T_{g,pHPMA} \approx 173$ °C), indicating a plasticizing effect of the Simvastatin molecules on the polymer matrix. Furthermore, the experimentally obtained value was highly similar to the value predicted by Fox's equation ($T_{g,Fox} = 76$ °C) (Fox, 1956), allowing for the calculation of T_g in miscible polymer blends based on their composition (pHPMA/Simvastain = 70 wt.%/30 wt.%). The observed small difference in the T_g values indicated the presence of weak, nearly negligible interactions between the drug and matrix. In addition, the fact that only one T_g value of the prepared solid dispersion was observed implies a homogeneous character of the

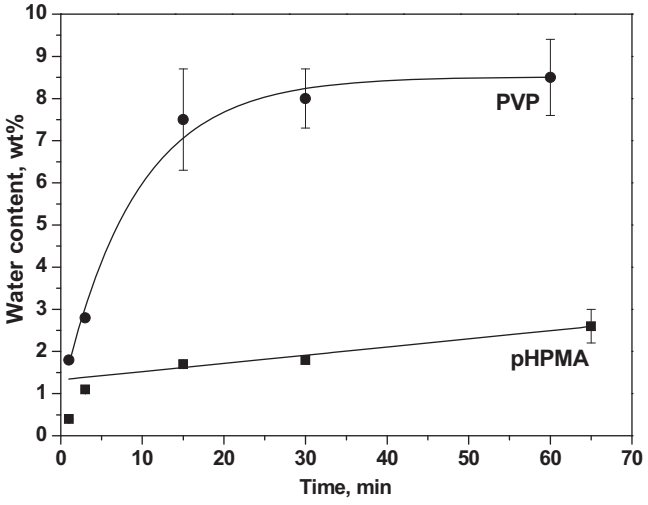

Fig. 1. Water sorption profiles of PVP (●) and pHPMA (■) obtained by thermogravimetric analysis; three replicate samples were used to obtain each data-point. The sorption profile of PVP was fitted to an exponential dependence, and the sorption profile of pHPMA was satisfactorily fitted to a linear dependence.

Table 1
Glass transition temperature values of Simvastatin, pHPMA and a 30/70 solid dispersion of the two (Sim_pHPMA).

Samples	Simvastatin	pHPMA	Sim_pHPMA
T_g (°C)	33	173	73
T_m (°C)	137	–	–

prepared system and a uniform distribution of the drug in the pHPMA matrix.

3.3. Raman spectroscopy

The glass transition temperature is one of the key parameters that can influence the product performance. However, molecular mobility of the drug, its miscibility with excipients, and the rate and extent of drug crystallization also significantly affect the properties of the drug formulation. In this respect, Raman spectroscopy and advanced techniques of ss-NMR spectroscopy are particularly suited to describe these molecular level processes leading to the formation of solid dispersions. Raman spectroscopy is a technique that is sensitive to the solid form of APIs and is capable of probing the sample at a molecular level, detecting changes in molecular structure, molecular conformation and packing (Chalmers, 2006; Graeser et al., 2008).

A strong fluorescent background and etaloning effect (Roper Scientific, Inc, 2000) was observed in the Raman spectrum of neat amorphous Simvastatin. These two phenomena were significantly suppressed when the drug was dispersed in pHPMA (Sim_pHPMA, Fig. 2c), and they were not present at all in the crystalline form of neat Simvastatin and neat pHPMA (Fig. 2a and d). The observed fluorescence was likely due to electronically excited states of Simvastatin molecules and their hydrogen bonded associates and not due to impurities (the impurities would have also fluoresced in the crystalline form and/or in the dispersion with the polymer). Because both systems formed slightly colored but transparent films, the observed fluorescence quenching could not be due to differences between the optical density of amorphous Simvastatin and its dispersion. Instead, the quenching was caused by molecular-level processes, such as a change in molecular conformation or intermolecular interactions due to: (i) the formation of Simvastatin crystalline domains in the polymer dispersion, (ii) the presence of small Simvastatin clusters (hydrogen bonded dimers or trimers) dispersed in the pHPMA matrix or (iii) the close molecular contact of the individual Simvastatin molecules with the pHPMA macromolecules, which may have acted as a quencher (Lackowicz, 2006). In such a case, the maximum distance between Simvastatin (the fluorophore) and pHPMA (the quencher) would be on the order of tens of Ångströms. Several mechanisms could lead to the quenching, and the present data are not sufficient to identify them.

A difference spectrum was obtained (Fig. 3) by subtracting the neat pHPMA spectrum from the Sim_pHPMA spectrum. The C—H and C=O stretching vibration regions of the difference spectrum were each compared with the spectra of neat crystalline Simvastatin and neat amorphous Simvastatin. The number of bands and their position in the C—H stretching vibration region were identical in the difference spectrum and amorphous drug spectrum. The relative intensity of the band at 2930 cm^{-1} in the difference spectrum was significantly higher, which was at least partially caused by the narrower half-width of this band. The observed line-width narrowing was likely caused by the increased ordering of the corresponding part of the Simvastatin molecule in the Sim_pHPMA dispersion when compared to the amorphous Simvastatin. In the C=O stretching vibration region of the crystalline Simvastatin and the dispersion (Fig. 2), there were several bands present that significantly varied in intensity. Only the highest intensity band at 1649 cm^{-1} was well resolved in the amorphous Simvastatin. The band was tentatively assigned to the C=O group of the ester in the aliphatic chain of a Simvastatin molecule (C18), which is involved in hydrogen bonding (Colthup et al., 1990). The structure of Simvastatin in the dispersion was closely related to the amorphous form, and the highest intensity band was also located at 1649 cm^{-1}. There were some differences

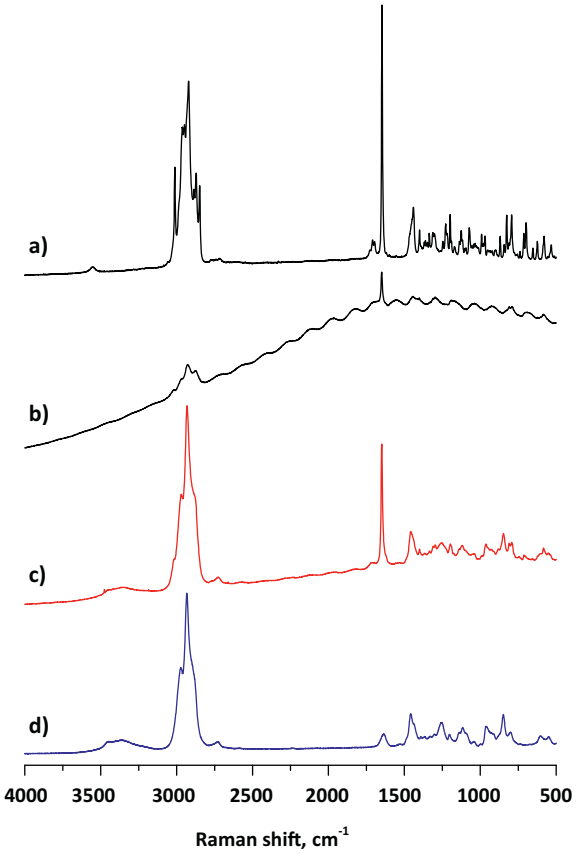

Fig. 2. Raman spectra of crystalline Simvastatin (a, dotted line), amorphous Simvastatin (b, full black line), a Sim_pHPMA solid dispersion (c, full red line), and neat pHPMA (d, full blue line). An excitation laser line of 632.8 nm was used. The spectra were scaled and offset for clarity. (For interpretation of the references to color in this figure legend, the reader is referred to the web version of this article.)

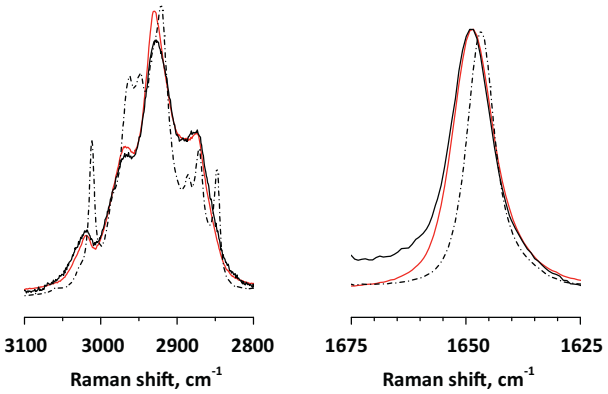

Fig. 3. The C—H stretching vibration region (left) and C=O stretching vibration region (right) of the Raman spectra of crystalline Simvastatin (dotted black line) and amorphous Simvastatin (full black line), as well as the difference spectrum created by the subtraction of the neat pHPMA spectrum from the 30/70 dispersion Sim_pHPMA spectrum (full red line). The spectra were scaled. (For interpretation of the references to color in this figure legend, the reader is referred to the web version of this article.)

between the amorphous and crystalline drug spectra (Fig. 3): the highest intensity band displayed a slight redshift to a lower wavenumber (1646 cm^{-1}) and a narrower line-width when in the crystalline state. It is possible that the carbonyl group can participate in slightly weaker hydrogen bonds when in the amorphous form, and there is also greater variability in the hydrogen bonding pattern. The similarities of the spectra of the amorphous Simvastatin and the Simvastatin in the dispersion suggest that the fluorescence reduction in the dispersion spectrum in Fig. 2 was not caused by the presence of crystalline domains. Instead, fluorescence of the dispersed drug was likely quenched by close molecular contact with the pHPMA macromolecules or with another Simvastatin molecule. Simoes et al. (2013) illustrated that even in the gas phase Simvastatin had the propensity to form intermolecular hydrogen bonds as opposed to intramolecular H-bonds. Therefore, the drug was likely molecularly mixed (in the form of monomers and hydrogen bonded dimers and trimers) with the polymer matrix.

3.4. Solid-state NMR spectroscopy

The suppression of the strong fluorescent background in the Raman spectra observed for Simvastatin dispersed in pHPMA poses questions concerning the morphology, intra- and intermolecular interactions, molecular clustering and segmental dynamics. In this respect, ss-NMR spectroscopy is one of the best-suited methods to obtain the required information at the atomic resolution, even for amorphous systems (Paudel et al., 2014). Although primary information regarding the structure and composition of the prepared solid dispersion can be gained from ^{13}C and ^{15}N CP/MAS NMR spectra, the segmental mobility is traditionally investigated using ^{1}H NMR line-width analysis, ^{13}C spin-lattice relaxation experiments and one-bond $^{1}H-^{13}C$ dipolar coupling measurements. A set of 2D $^{1}H-^{13}C$ FSLG HETCOR correlation spectra was recorded to probe the homogeneity of the systems at the nanometer scale.

3.4.1. ^{13}C and ^{15}N CP/MAS NMR spectroscopy

Considerable structural changes of Simvastatin upon the formation of a solid dispersion with pHPMA were clearly observed in the ^{13}C CP/MAS NMR spectra (Fig. 4), which provide a comparison of neat substances with the final product. The signal assignment was performed based on previous NMR studies (Brus and Jegorov, 2004; Nunes et al., 2014). Predominantly, the observed broadening of the Simvastatin signals clearly indicated its complete amorphization, and no residues of crystalline Simvastatin were found in the Sim_pHPMA solid dispersion. However, this result is only one indicator of practical applicability of a drug–polymer solid dispersion. The second and likely more important indicator is its long-term physical stability, i.e., the prevention of phase transitions.

In this respect, the glass transition temperature is widely recognized as an important descriptor of potentially applicable amorphous systems: one often-quoted rule of thumb is that crystallization will be negligible if a sample is stored 50 °C below its T_g (Hancock et al., 1995). The relationship between the stability and temperature relative to T_g is not often easily predictable, particularly for multi-component systems; hence, individual systems should be thoroughly evaluated. In the Sim_pHPMA dispersion studied in this work, the spectra recorded over two years indicated no changes in the structure when stored at laboratory temperature, although the glass transition temperature was approximately 73 °C (Supporting information).

An in-depth inspection of the line shapes of the ^{13}C CP/MAS NMR spectra revealed additional differences in each segment of

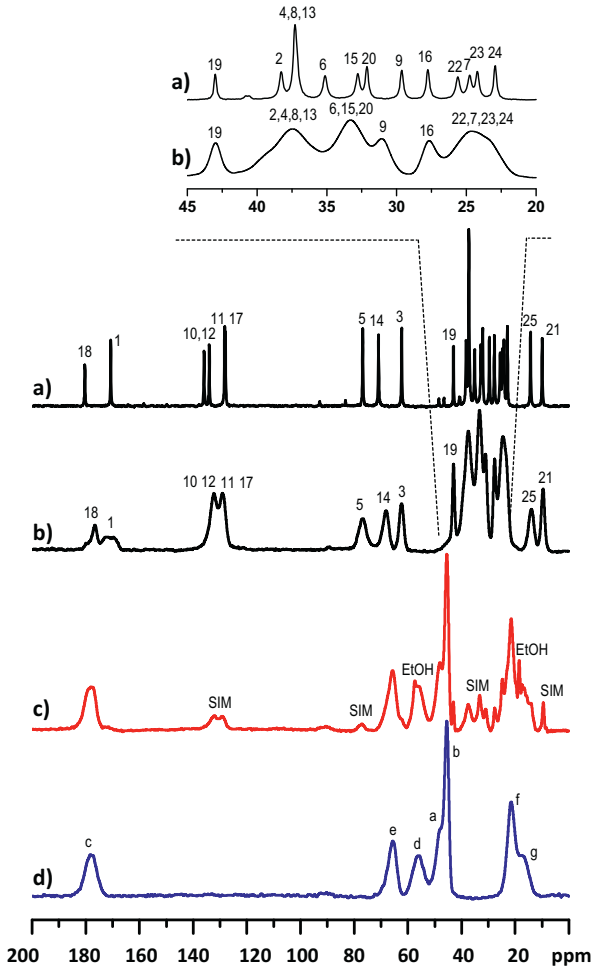

Fig. 4. ^{13}C CP/MAS NMR spectra of neat crystalline and amorphous Simvastatin (black lines (a) and (b), respectively), the Sim_pHPMA solid dispersion (red line, c) and neat pHPMA (blue line, d). (For interpretation of the references to color in this figure legend, the reader is referred to the web version of this article.)

the Simvastatin molecules incorporated into the pHPMA matrix. In particular, the signals corresponding to the ester substituent and lactone ring of Simvastatin were narrower in the solid dispersion than in the neat amorphous state (Fig. 5). In contrast, no signal narrowing was observed in the region of naphthalene rings. A narrower NMR signal typically indicates a more ordered or more mobile molecular segment. Thus, this observation can be attributed to the increase in dynamics and/or order of the ester and lactone components of Simvastatin molecules when incorporated into a pHPMA matrix, whereas the naphthalene ring remained relatively rigid.

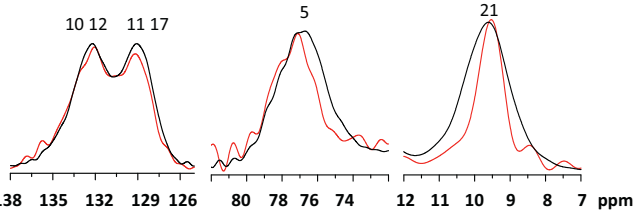

Fig. 5. Comparison of the ^{13}C CP/MAS NMR spectra of neat amorphous Simvastatin (black line) and the 30/70 Sim_pHPMA dispersion (red line). The spectra were scaled. (For interpretation of the references to color in this figure legend, the reader is referred to the web version of this article.)

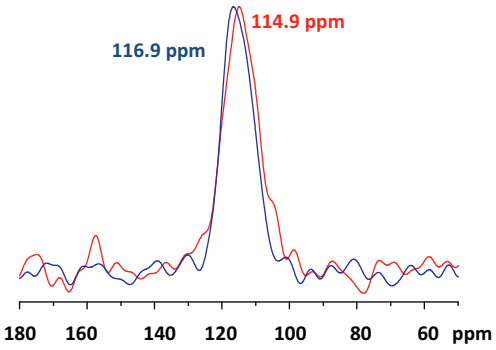

Fig. 6. ^{15}N CP/MAS NMR spectra of pHPMA (blue line) and the 30/70 Sim_pHPMA dispersion (red line). (For interpretation of the references to color in this figure legend, the reader is referred to the web version of this article.)

The possible involvement of the —NH—CO— moieties of pHPMA in the formation of hydrogen bonds with Simvastatin was investigated using ^{15}N CP/MAS NMR spectroscopy. A change in hydrogen bonding of the NH group is typically expected to induce changes in the corresponding ^{15}N NMR signal (Li et al., 2006; Song et al., 2013). However, in the case of the Sim_pHPMA dispersion, only a slight decrease in the ^{15}N NMR chemical shift was observed (approximately 2 ppm; Fig. 6), indicating a nearly negligible weakening of the hydrogen bonding of the pHPMA amide group in the solid dispersion. Thus, this finding suggests that the structure and dynamics of the polymer chains in the pHPMA matrix at room temperature were not considerably involved with the incorporated Simvastatin molecules.

3.4.2. ^{1}H MAS NMR and $T_1(^{13}C)$ and $T_{1\rho}(^{13}C)$ relaxation – segmental dynamics

The most straightforward method of investigating segmental motions by ss-NMR is to measure the static ^{1}H NMR spectra. The broad lines in the ^{1}H NMR spectra of dynamically heterogeneous (e.g., semicrystalline) polymers consist of several spectral components related to segments with different mobility (Olcak et al., 2004; Spevacek and Brus, 1999). The narrow lines typically correspond to the flexible molecular segments that are considerably above the glass transition, whereas the broad signals reflect rigid segments within the crystalline or amorphous glassy domains far below T_m and T_g, respectively. The same two-component behavior with a narrow signal that is superimposed on the broad line is reflected in the static ^{1}H NMR spectrum of the Sim_pHPMA solid dispersion (red line, Fig. 7). However, the glass transition temperature of the system ($T_{g,\,Disp}$ = 73 °C) was clearly above the measurement temperature. Thus, understanding this phenomenon requires the entire spectrum of all modes of segmental motions to be considered.

The molecular mobility responsible for the glass transition is called the "global mobility", and the molecular motions involved in the transition are referred to as alpha (α)-relaxation motions. The α-relaxation processes are attributed to molecular rotations and translations, and their frequency can vary over several orders of magnitude when the temperature of the system is increased from below T_g to above T_g. Because α-relaxations are present across a temperature interval over which the sample can transform from a low mobility system (just below T_g) to a considerably higher mobility system (above T_g), the global mobility has been thought to be the determining factor in the tendency of the polymer to crystallize. Amorphous systems can also exhibit intra-molecular reorientations referred to as beta (β)-relaxation motions and commonly described as secondary relaxations or the "local mobility" (Bhattacharya and Suryanarayanan, 2009). The secondary relaxations, often coupled with α-relaxations, can be a result of rotation about chemical bonds or even of the motion of entire molecules. These secondary relaxations were observed by Johari and Goldstein for completely rigid molecules and are known as Johari–Goldstein (JG) relaxations (Johari and Goldstei, 1970). β-Relaxations occur on a faster timescale than α-relaxations, are non-cooperative in nature, and obey Arrhenius kinetics below T_g. In Fig. 7, the static ^{1}H NMR spectra were obtained at laboratory temperature, i.e., below the T_g of the Sim_pHPMA solid dispersion (73 °C, Table 1). Therefore, the narrow signal was likely related to β-relaxations in the system studied. The smaller Simvastatin molecules are capable of these fast, non-cooperative motions, giving rise to the narrow signal, whereas the broad line reflected the rigid pHPMA segments.

The temperature-dependent ^{1}H MAS solid-state NMR spectra (Fig. 8) of amorphous Simvastatin and a dispersion of Sim_pHPMA illustrate that the behavior of neat amorphous Simvastatin upon heating was comparable with data from the literature (Nunes et al., 2014). The signals occurring at and above approximately 5 ppm were clearly resolved at 81 °C in neat Simvastatin, and the temperature-induced line-width reduction indicated a shortened correlation time (Nunes et al., 2014). The same effect was observed in the solid dispersion Sim_pHPMA at approximately 53 °C, i.e., at a temperature 30 °C lower than in neat amorphous Simvastatin. As recently revealed by dielectric relaxation spectroscopy, the

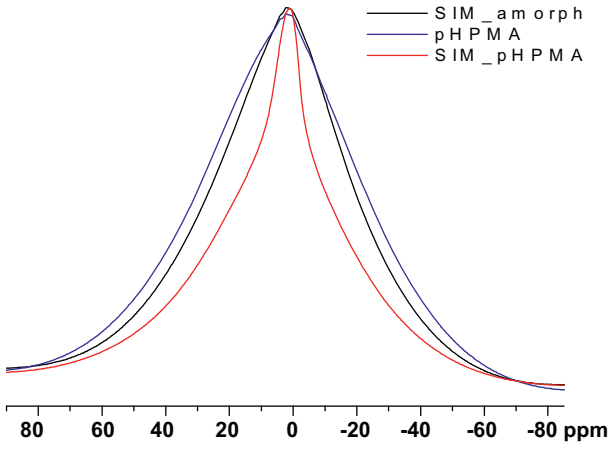

Fig. 7. Static ^{1}H NMR spectra of neat amorphous Simvastatin (black line), pHPMA (blue line) and the 30/70 Sim_pHPMA dispersion (red line). (For interpretation of the references to color in this figure legend, the reader is referred to the web version of this article.)

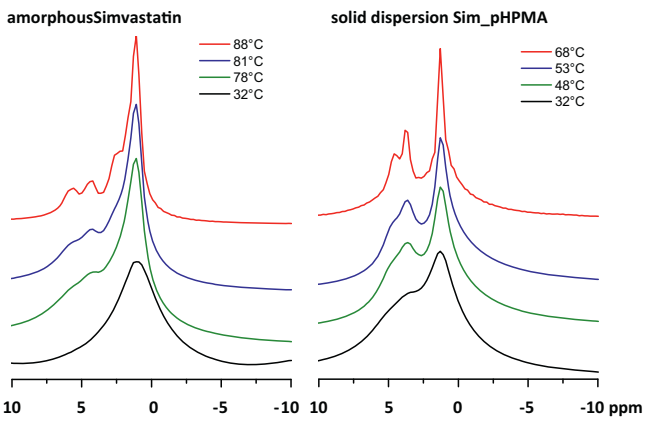

Fig. 8. Variable-temperature ^{1}H MAS NMR spectra of neat amorphous Simvastatin (left) and the solid dispersion of Simvastatin in pHPMA (right) obtained at a rate of 6 kHz.

Table 2
$T_1(^{13}C)$ spin-lattice relaxation times obtained at 303 K for neat amorphous Simvastatin, pHPMA and the 30/70 dispersion Sim_pHPMA.

Group (atoms)	$T_1(^{13}C)$ (s)						
	CH, C (nos. 10, 12,11, 17)	CH (e)	CH_2 (d)	CH (b)	CH_3 (no. 19)	CH_2,CH (nos. 6 and 20)	CH_3 (no. 21)
Sim_amorph	18.0				6.9	3.3	1.1
pHPMA		4.7	25.5	12.1			
Sim_pHPMA	20.9	2.9	14.9	11.2	6.3	2.1	1.5

Table 3
$T_1(^{13}C)$ spin-lattice relaxation times obtained at 333 K for neat amorphous Simvastatin, pHPMA and the 30/70 dispersion Sim_pHPMA.

Group (atoms)	$T_1(^{13}C)$ (s)						
	CH, C (nos. 10, 12, 11, 17)	CH (e)	CH_2 (d)	CH (b)	CH_3 (no. 19)	CH_2, CH (nos. 6 and 20)	CH_3 no. (21)
Sim_amorph	22.3				7.2	3.7	1.3
pHPMA		2.5	20.3	11.2			
Sim_pHPMA	22.5	1.5	10.4	10.1	6.6	0.8	1.2

segmental motions associated with the glass transition of amorphous Simvastatin (i.e., large amplitude cooperative motions, T_g(Sim) = 33 °C) are related to the main relaxation processes (Nunes et al., 2014). Thus, the dramatic narrowing and splitting of the ^{1}H MAS NMR signals observed in the variable-temperature experiment (Fig. 8) allow us to identify a critical temperature (T_c), around which the high-amplitude isotropic motions are considerably released and their frequencies reach the frequency window of the ^{1}H NMR experiment (approximately 500 MHz), rather than T_g (Williams et al., 1955).

As demonstrated in Fig. 8, the critical temperature of neat amorphous Simvastatin was approximately 80 °C, whereas the critical temperature considerably decreased to approximately 50 °C when Simvastatin was incorporated into the pHPMA matrix. The temperature depression of approximately 30 °C clearly indicates smaller steric restrictions of Simvastatin molecules in the Sim_pHPMA dispersion. Thus, Simvastatin molecules in a glassy state in the neat amorphous drug appear to be tightly packed and mutually interacting via non-covalent interactions. Such packing and intermolecular interactions were considerably weakened in the solid dispersions, which implies that the Simvastatin molecules occupy voids with considerably larger free volume. However, the enhanced reorientation freedom of Simvastatin molecules in the solid dispersion could allow easier crystallization. However, no crystallization was observed when the samples were tested over two years.

More detailed insight into the segmental dynamics of the studied system was provided by NMR spin-relaxation measurements, which examine segmental motions at two distinct time scales. The laboratory reference frame $T_1(^{13}C)$ relaxation time is sensitive to the high-frequency motions of small segments (librations, rotations and flip-flops) in the order of hundreds of MHz, whereas the rotating reference frame $T_{1\rho}(^{13}C)$ relaxation time is sensitive to large segmental motion (the entire molecular chains or supra molecular assemblies) in the mid-kilohertz range (tens of kHz).

To probe the effect of the polymer matrix on the behavior of the drug molecules and vice versa, the $T_1(^{13}C)$ and $T_{1\rho}(^{13}C)$ relaxation times were measured at various temperatures (Tables 2–5; see also the Supporting information for a schematic dependence between the relaxation times and frequency motions, as well as correlation times). As follows from the analysis of the $T_1(^{13}C)$ relaxation times (Tables 2 and 3), no significant changes in the high-frequency (MHz) motions of the Simvastatin molecules occurred when they were incorporated into the polymer matrix. Similarly, in the prepared solid dispersion, the pHMPA backbone dynamic was not affected by the presence of Simvastatin molecules. A slight increase in the rate of the high-frequency motions can be expected in the pHPMA side-chains, as reflected by the observed decrease of the corresponding $T_1(^{13}C)$ relaxation times.

However, considerably stronger effects were observed when probing the mid-kHz motions. As reflected by the considerable decrease in the $T_{1\rho}(^{13}C)$ relaxation times found for the ethylene linker and ester substituent of Simvastatin, the rate of these motions increased considerably after incorporation into the polymer matrix. Similarly, the decrease in the $T_{1\rho}(^{13}C)$ relaxation times of the naphthalene rings indicates a slight increase in the global dynamics of the Simvastatin molecules. In contrast, the segmental motions of the pHPMA chains in the Sim_pHPMA dispersion were not affected by the presence of Simvastatin.

3.4.3. ^1H—^{13}C dipolar couplings – motional amplitudes

For detail probing and clear visualization of the dynamical heterogeneities in the prepared system, we focused on the measurements of motional amplitudes. This investigation was experimentally achieved via the ^{1}H—^{13}C separated-local-filed AMPISEMA experiment, allowing for domain- and site-specific measurements of the ^{1}H—^{13}C dipolar couplings (Brus et al., 2008). Any molecular motion with a correlation time shorter than approximately 40 μs causes averaging of the one-bond ^{1}H—^{13}C dipolar interactions. Then, the ratio of the motionally averaged dipolar coupling constant (D_{CH}) and the rigid-limit value ($D_{CH,rig}$ = 23.1 kHz for a C—H bond of 1.09 Å) defines the order parameter (S) that can be converted to the amplitude of segmental motion (Palmer et al., 1996). In general, the order parameter S is a measure of the equilibrium distribution of orientations of the bond vector

Table 4
$T_{1\rho}(^{13}C)$ spin-lattice relaxation times obtained at 303 K for neat amorphous Simvastatin, pHPMA and the 30/70 dispersion Sim_pHPMA.

Group (atoms)	$T_{1r}(^{13}C)$ (ms)						
	CH, C (nos. 10, 12, 11, 17)	CH (e)	CH_2 (d)	CH (b)	CH_3 (no. 19)	CH_2, CH (nos. 6 and 20)	CH_3 (no. 21)
Sim_amorph	7.7				85.7	5.1	27.9
pHPMA		3.8	1.0	16.7			
Sim_pHPMA	5.4	3.6	1.1	16.0	41.7	2.9	19.0

Table 5
$T1\rho(^{13}C)$ spin-lattice relaxation times obtained at 333 K for neat amorphous Simvastatin, pHPMA and the 30/70 dispersion Sim_pHPMA.

group (atoms)	$T_{1r}(^{13}C)$ (ms)						
	CH, C (nos. 10, 12, 11, 17)	CH (e)	CH_2 (d)	CH (b)	CH_3 (no. 19)	CH_2, CH (nos. 6 and 20)	CH_3 (no. 21)
Sim_amorph	4.2				32.8	2.5	15.7
pHPMA		2.8	1.0	10.0			
Sim_pHPMA	3.5	1.5	1.0	10.1	16.6	0.8	10.2

μ(t) (e.g., C—H bond) in a molecular reference frame and ranges from 1 for a fixed orientation to 0 for free motion (Lipari and Szabo, 1982; Palmer et al., 1996) In the simplest case, assuming a small-amplitude (θ) axially symmetric motion (so that $\langle\sin\theta\rangle \approx \langle\theta\rangle$), the order parameter can be converted to the average fluctuation angle of the C—H segment $\sqrt{\langle\theta^2\rangle}$ (root mean square amplitude, r.m.s.) according to the following relation: $S = 1 - 3/2\langle\theta^2\rangle$.

In our particular case, the order parameters (Table 6) were estimated from the dipolar profiles extracted from the $^1H—^{13}C$ AM-PISEMA spectra (Fig. 9a) for the CH and CH_2 groups representing typical molecular segments. The pHPMA backbone and side-chain dynamics were characterized through the CH_2 groups *a* and *d* (Scheme 1 and Fig. 9c). The segments of the naphthalene rings (nos. 11 and 17), lactone cycle (no. 5) and ester substituent (no. 20) were used to characterize the motional amplitudes of Simvastatin (Fig. 9b and c).

However, the $^1H—^{13}C$ dipolar profile of the ester substituent that allows for diagnostics of a high-amplitude rotation motion of Simvastatin (Brus and Jegorov, 2004) was overlapped by two other signals (CH_2 units nos. 6 and 15). Therefore, we focused on identifying the precise ^{13}C resonance frequency of this unit. For this task, we used a ^{13}C CPPI NMR experiment that suppresses and inverts the signals of the rigid CH and CH_2 units, respectively, while maintaining the positive signals of mobile segments (Wu et al., 1994). Thus, the positive signal detected at 33 ppm could be unambiguously attributed to the rapidly rotating CH_2 group no. 20 (see Supporting information for the spectra). Thus, considering the overlap with the dipolar profiles of CH_2 units nos. 6 and 15 (Fig. 4), the order parameter for the ester substituent was estimated from the inner splitting of the dipolar profile (Fig. 9d), and the outer splitting was attributed to the more rigid CH_2 units nos. 6 and 15.

As demonstrated in the order parameters determined for pHPMA, the incorporation of Simvastatin molecules had no detectable impact on motional amplitudes of the backbone segments (CH_2*a*,*S* = 0.96). Assuming the simplest approach, the order parameter was converted to the r.m.s. angular fluctuation, which was 9° for the pHPMA backbone in the neat amorphous state, as well as in the Sim_pHPMA solid dispersion. Slightly higher amplitudes were found for the side-chain reorientations in neat pHPMA, reaching 10.4° for CH_2 segment *d*; however, negligible changes in the r.m.s. angular fluctuations were found upon Simvastatin incorporation.

In contrast, the dynamical behavior of Simvastatin is fundamentally more complex even in the neat amorphous state. Although the naphthalene ring and lactone cycle are relatively rigid with r.m.s. values of 16.2° (*S* = 0.88, =CH nos. 17 and 11) and 18.6° (*S* = 0.84, CH no. 5), respectively, the ester substituent executed fast high-amplitude rotations and/or discrete jumps, as reflected by the low order parameter *S* = 0.62 (CH_2 no. 20). By incorporating Simvastatin into the pHPMA matrix, the inner doublet disappeared and a broad central signal emerged in the zero-frequency position (Fig. 9d), counterintuitively indicating that the angular fluctuations of the ester tail of Simvastatin were enhanced. The order parameter estimated from the half-width of the broad central signal reached *S* = 0.41. The decrease in the order parameter observed for the naphthalene ring and lactone cycle was considerably smaller, as indicated by the increase in the r.m.s. amplitudes to 22.4° and 23.4°, respectively.

Thus, the current analysis highlights that the dynamical heterogeneities of Simvastatin molecules exist not only in the neat amorphous state (Nunes et al., 2014) but also in the solid dispersion with a pHPMA matrix. Moreover, it was confirmed that global reorientation of the Simvastatin molecules, as well as the internal rotation of the ester substituent, was enhanced upon dispersion in the pHPMA matrix. In contrast, despite the higher free volume introduced by Simvastatin into the polymer matrix, as reflected by the reduced T_g, no considerable enhancement in the segmental dynamics of pHPMA was observed at room temperature. The observed increase in the motional freedom determined by relaxation and separated-local-field experiments, as well as corroborated by ^1H MAS NMR spectroscopy, indicates a greater free volume of the Simvastatin molecules in the dispersion compared with the neat amorphous state. These findings lead to the questions regarding the homogeneity of the system and the distribution of Simvastatin molecules along the polymer chains.

3.4.4. $T_1(^1H)$, $T_{1\rho}(^1H)$ and $^1H—^{13}C$ HETCOR experiments – clustering of Simvastatin molecules

When analyzing the homogeneity of multi-component solids, ss-NMR spectroscopy traditionally relies on the measurement of the $^1H—^1H$ spin diffusion. There are numerous ss-NMR techniques

Table 6
Order parameters (*S*) and r.m.s. angular fluctuations $\left(\sqrt{\langle\theta^2\rangle}\right)$ calculated from dipolar profiles extracted from the $^1H—^{13}C$ AM-PISEMA spectra.

	Simvastatin naphthalene ring (no. 17)		Simvastatin ester tail (no. 20)		Simvastatin lactone (no. 5)		pHPMA side chain (*d*)		pHPMA main chain (*a*)	
	S	$\sqrt{\langle\theta^2\rangle}$deg	*S*	$\sqrt{\langle\theta^2\rangle}$ deg	*S*	$\sqrt{\langle\theta^2\rangle}$deg	*S*	$\sqrt{\langle\theta^2\rangle}$ deg	*S*	$\sqrt{\langle\theta^2\rangle}$deg
Sim am	0.88	16.2	0.62	28.8	0.84	18.6	–	–	–	–
Sim cryst	0.99	2.3	0.44	35.0	0.97	8.0	–	–	–	–
pHPMA	–	–	–	–	–	–	0.95	10.4	0.96	9.0
Sim_pHPMA	0.77	22.4	0.41	35.8	0.75	23.4	0.94	11.0	0.96	9.0

To calculate the order parameter $S = \nu_{CH}/\nu_{CH,rig}$, the rigid-limit value $\nu_{CH,rig}$ = 13.4 kHz corresponding to the dipolar coupling constant $D_{CH,rig}$ = 23.1 kHz (C—H distance 1.09 Å) was applied. The relationship between dipolar coupling constants and the splitting of dipolar profiles is the following: $\Delta\nu_{CH} = \sin 54.7 D_{CH,rig}/\sqrt{2}$.

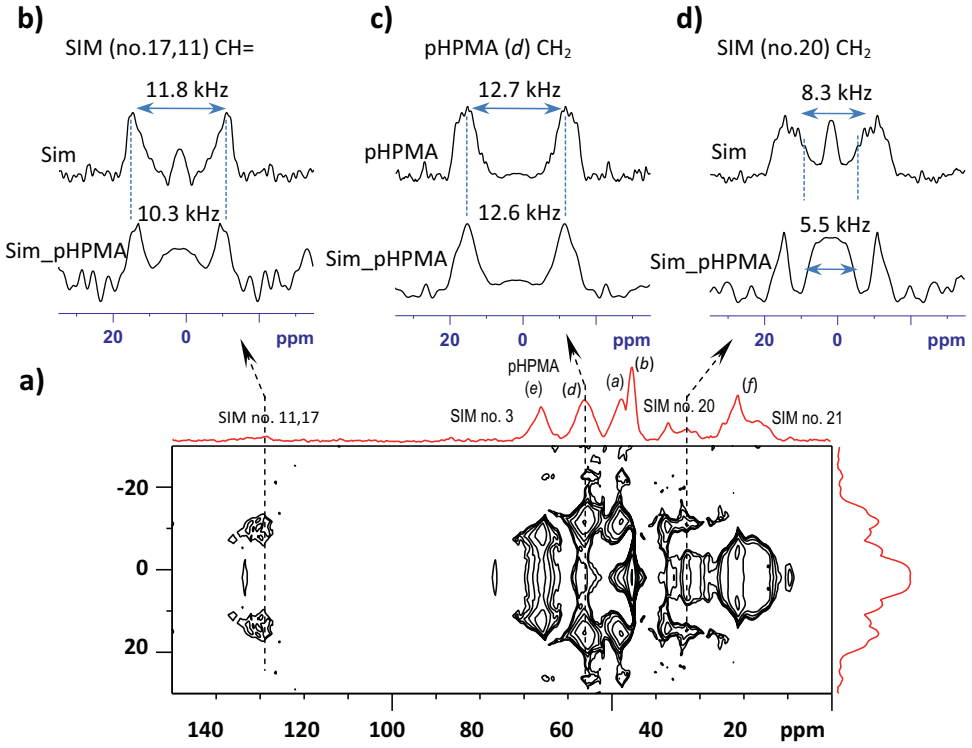

Fig. 9. 2D $^{1}H-^{13}C$ SLF-AM-PISEMA NMR spectrum of the Sim_pHPMA solid dispersion (a); dipolar profiles extracted for CH_2 group *d* of pHPMA (b); CH_2 group no. 20 (c); and CH= units nos. 11 and 10 of Simvastatin (d). The dipolar profiles were extracted for neat components (upper spectra) and the Sim_pHPMA solid dispersion (bottom spectra).

(Caravatti et al., 1985; Clauss et al., 1993; Vogt et al., 2013) that allow the domain sizes to be estimated from approximately 1 to 500 nm. The most robust technique is based on measurements of the ^{13}C-detected ^{1}H spin-lattice relaxation times in the laboratory and rotating frame, $T_1(^{1}H)$ and $T_{1\rho}(^{1}H)$, respectively.

It was demonstrated that for a wide range of two-component and multi-component polymer systems, differences in the ^{1}H relaxation times between the individual components typically indicate a heterogeneous character of the system (Vogt et al., 2009). However, in our case, the $T_1(^{1}H)$ values determined for the neat crystalline and amorphous Simvastatin and the neat pHPMA were nearly identical ($T_1(^{1}H)$ = 1.5, 1.4 and 1.0 s, respectively), disallowing reliable interpretation. Thus, we focused on the analysis of the $T_{1\rho}(^{1}H)$ spin-lattice relaxation times. The values for the neat crystalline and neat amorphous Simvastatin differed considerably from those for the neat pHPMA (Table 7). In the Sim_pHMPA solid dispersions, the $T_{1\rho}(^{1}H)$ spin-lattice relaxation times determined for the dispersed Simvastatin and for the pHPMA matrix were nearly identical and were located between the values for the neat components. This finding indicates that the system was homogenous in the scale of tens of nanometers and that the domain size of Simvastatin in the pHPMA matrix is not larger than several nanometers.

The most critical limitation for reliable interpretation of the above-mentioned procedure is the assumption that the segmental dynamics of both components in the neat state are not considerably changed in the solid dispersion. However, this assumption was not true in the prepared Sim_pHPMA system, as indicated above. Consequently, to more precisely determine the homogeneity level, we utilized $^{1}H-^{13}C$ FSLG HETCOR NMR spectroscopy, which allows the ^{1}H polarization transfer to be traced for each component and molecular segment that was resolved according to the ^{13}C NMR chemical shift.

As recently demonstrated, the simple Hartman–Hahn (HH) CP step enables relatively fine control over the distance at which the ^{1}H magnetization is transferred. Typically, most correlations observed at HH-CP contact times <110–150 μs (t_m) correspond to $^{1}H-^{13}C$ distances <2.5 Å, whereas the medium-range $^{1}H-^{13}C$ contacts of approximately 3.0 Å typically requires 300 μs (Harper et al., 2007). This case is clearly demonstrated in the $^{1}H-^{13}C$ FSLG HETCOR NMR spectrum of neat amorphous Simvastatin, in which the correlation signals between Simvastatin –CH= protons nos. 10 and 17 (δ_{1H} = 6 ppm) and carbon atoms nos. 9 and 16, separated by approximately 2.2 Å, were well evolved (Fig. 10, black contours). Thus, the cross-peaks related to inter-component transfer between the pHPMA segments and Simvastatin molecules detected in the $^{1}H-^{13}C$ FSLG HETCOR NMR spectrum measured under identical conditions (Fig. 10, red contours) indicate relatively close intermolecular contacts and exclude extensive phase separation.

However, because the complete evolution of these pHPMA–Simvastatin correlation signals was attained after t_{eq} = 1100 μs, the Simvastatin molecules clearly form local clusters. By applying the generally accepted model, (Schmidt-Rohr et al., 1992) the polarization transfer pathway (x) was estimated using the following equation:

$$x = \frac{\varepsilon}{f_{pol}}\sqrt{\frac{4D_{eff}t_{eq}}{\pi}} \quad (1)$$

where D_{eff} is effective spin-diffusion coefficient, t_{eq} is the equilibrium spin-exchange mixing time (t_{eq} = 1,100 μs), f_{pol} is

Table 7
$T_1(^{1}H)$ and $T_{1\rho}(^{1}H)$ spin-lattice relaxation times obtained for crystal simvastatin, pHPMA and the 30/70 dispersion of simvastatin in pHPMA.

	$T_1(^{1}H)$, s API (nos. 2, 4, 8, 13)	$T_1(^{1}H)$, s polymer (a, b)	$T_{1\rho}(^{1}H)$, ms API (nos. 2, 4, 8, 13)	$T_{1r}(^{1}H)$, ms polymer (a, b)
Sim_crystal	1.5	–	270	–
Sim_amorph	1.4	–	16	–
pHPMA	–	1	–	4.5
Sim_pHPMA	1.3	1.3	4.8	4.8

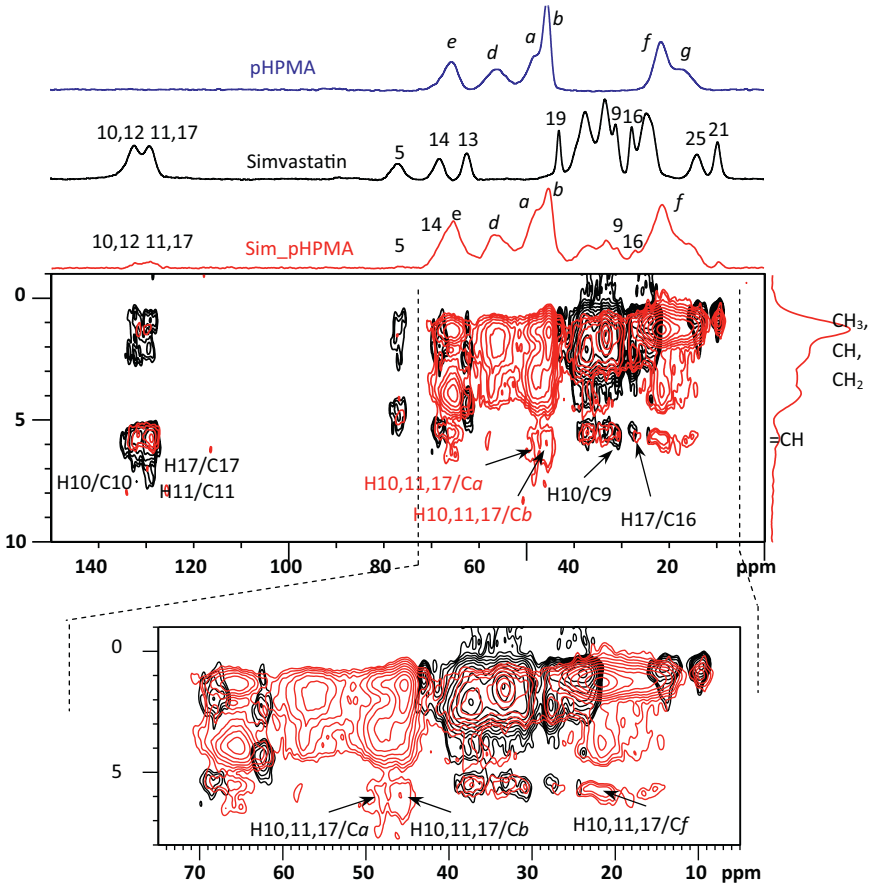

Fig. 10. 2D $^{1}H-^{13}C$ HETCOR correlation spectra of the prepared Sim_pHPMA solid dispersion (red contours) and neat amorphous Simvastatin (black contours) measured at a cross-polarization mixing time of 300 μs. (For interpretation of the references to color in this figure legend, the reader is referred to the web version of this article.)

the volume fraction of the polymer matrix (f_{pol} = 0.7, assuming a similar density for amorphous Simvastatin and pHPMA), and ε = 1–3 is the scaling factor that reflects the dimensionality of the spin-diffusion process. The effective spin-diffusion coefficient D_{eff} = 0.19 $nm^2\,ms^{-1}$ was calculated from the half-width of the static ^{1}H NMR spectrum ($\Delta\nu$ = 28 kHz; Fig. 7) according to the following relationship:

$$D_{eff} = \frac{1}{12}\sqrt{\frac{\pi}{2\ln 2}}\langle r^2\rangle \Delta\nu_{1/2} \quad (2)$$

where $\langle r^2\rangle$ is the mean-square distance between the nearest spins (typically r = 0.20–0.25 nm) and $\Delta\nu_{1/2}$ is the full width at half intensity of the ^{1}H NMR signals. Then, assuming a three-dimensional geometry of the spin-diffusion process proceeding from the spherical particles of dispersed Simvastatin (ε = 3), the calculated characteristic diffusive pathway is approximately 2.0–2.5 nm. Considering the effective size (Brus et al., 2004; Jia et al., 2003) of a Simvastatin molecule $x_{Sim} = (l \times d)^{0.5}$ = 1.1 nm (Fig. 11), the obtained characteristic dimension indicates the formation of nanosized domains in the Sim_pHPMA system that could consist of 2–4 molecules of Simvastatin (Fig. 11).Overall, the obtained results imply the formation of a nano-heterogeneous solid solution/suspension containing nanosized clusters of Simvastatin dispersed in a rigid pHPMA matrix. This finding explains the negligible tendency of Simvastatin to crystallize in the polymer matrix. Although the molecular mobility of Simvastatin enhances the ability to find the proper conformation and packing, the clusters of Simvastatin are not sufficiently large to effectively crystallize. Moreover, the pHPMA polymer chains are sufficiently rigid to form a glassy phase, effectively preventing translation diffusion of Simvastatin molecules, coalescence of Simvastatin clusters and growth of Simvastatin domains. Thus, the prepared solid dispersion of Sim_pHPMA is a physically stable system, exhibiting an unchanged structure over the two-year course of this study.

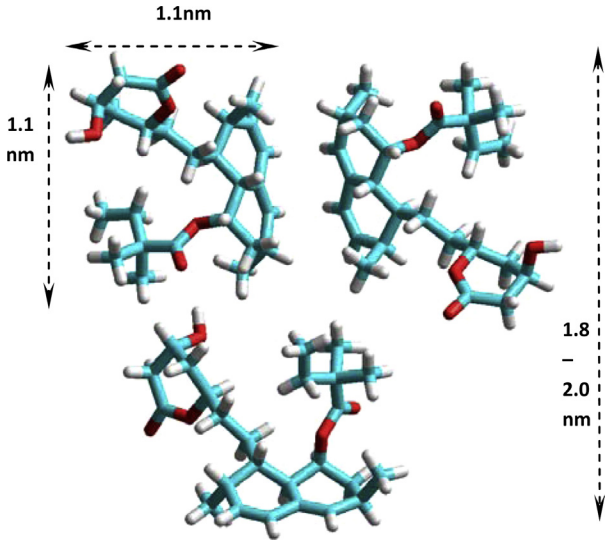

Fig. 11. Idealized structure of the Simvastatin domains dispersed in the pHPMA matrix (the trimeric motif was extracted from the crystal structure of Simvastatin (Cejka et al., 2003)).

4. Conclusions

A new type of completely amorphous solid dispersion of Simvastatin molecules in pHPMA was prepared. As demonstrated by a range of DSC, XRPD, Raman and ss-NMR experiments, including fluorescence analysis in Raman spectra, Simvastatin was found to form nanosized clusters of approximately 2–3 nm dispersed in the rigid, glassy pHPMA matrix. Furthermore, the segmental motion and global reorientation of the Simvastatin molecules increased upon dispersion in the pHPMA matrix, whereas the segmental dynamics of the pHPMA chains was unaffected. Due to the considerably reduced kinetics of water sorption, the chosen polymer can more effectively protect Simvastatin or other sensitive drugs against chemical decomposition caused by long-term exposure to residual water present in the polymer matrix. Moreover, due to the strong inter-residual hydrogen bonding, the highly rigid pHPMA polymer chains form glassy barriers that inhibit the translation diffusion of Simvastatin molecules, the formation of large domains and subsequent crystallization. Thus, the prepared dispersion can be viewed as a nano heterogeneous glassy solution/suspension, the glass transition temperature of which ($T_g \approx 73\,^{\circ}C$) ensures suitable preconditions for the storage and application of amorphous drugs with low T_g. Systems exploiting pHPMA as a matrix are proving to be more suitable than, e.g., PVP for dispersion of APIs with glass transition near laboratory temperature.

Acknowledgements

The authors thank Czech Science Foundation (grant no. 14-03636S) and COST Action MP1202HINT (Ministry of Education, Youth and Sports LD14010) for financial support.

Appendix A. Supplementary data

Supplementary data associated with this article can be found, in the online version, at http://dx.doi.org/10.1016/j.ijpharm.2014.12.007.

References

Al-Obaidi, H., Ke, P., Brocchini, S., Buckton, G., 2011. Characterization and stability of ternary solid dispersions with PVP and pHPMA. Int. J. Pharm. 419, 20–27.
Ambike, A.A., Mahadik, K.R., Paradkar, A., 2005. Spray-dried amorphous solid dispersions of simvastatin, a low T-g drug: in vitro and in vivo evaluations. Pharm. Res. 22, 990–998.
Bhattacharya, S., Suryanarayanan, R., 2009. Local mobility in amorphous pharmaceuticals-characterization and implications on stability. J. Pharm. Sci. 98, 2935–2953.
Brough, C., Williams III, R.O., 2013. Amorphous solid dispersions and nano-crystal technologies for poorly water-soluble drug delivery. Int. J. Pharm. 453, 157–166.
Brus, J., 2000. Heating of samples induced by fast magic-angle spinning. Solid State Nucl. Magn. Reson. 16, 151–160.
Brus, J., Jegorov, A., 2004. Through-bonds and through-space solid-state NMR correlations at natural isotopic abundance: signal assignment and structural study of simvastatin. J. Phys. Chem. A 108, 3955–3964.
Brus, J., Urbanova, M., 2005. Selective measurement of heteronuclear H-1–C-13 dipolar couplings in motionally heterogeneous semicrystalline polymer systems. J. Phys. Chem. A 109, 5050–5054.
Brus, J., Spirkova, M., Hlavata, D., Strachota, A., 2004. Self-organization, structure, dynamic properties, and surface morphology of silica/epoxy films as seen by solid-state NMR, SAXS, and AFM. Macromolecules 37, 1346–1357.
Brus, J., Urbanova, M., Strachota, A., 2008. Epoxy networks reinforced with polyhedral oligomeric silsesquioxanes: structure and segmental dynamics as studied by solid-state NMR. Macromolecules 41, 372–386.
Brus, J., Urbanova, M., Sedenkova, I., Brusova, H., 2011. New perspectives of F-19 MAS NMR in the characterization of amorphous forms of atorvastatin in dosage formulations. Int. J. Pharm. 409, 62–74.
Caravatti, P., Neuenschwander, P., Ernst, R.R., 1985. Characterization of heterogeneous polymer blends by 2-dimensional proton spin diffusion spectroscopy. Macromolecules 18, 119–122.
Cejka, J., Kratochvil, B., Cisarova, I., Jegorov, A., 2003. Simvastatin. Acta Crystallogr. Sect. C: Cryst. Struct. Commun. 59, O428–O430.
Chalmers, J.M., 2006. The role of infrared and Raman spectroscopy in the solid-state characterization of pharmaceuticals. In: Zakrzewski, A., Zakrzewski, M. (Eds.), Solid State Characterization of Pharmaceuticals. Pergamon, Poland, pp. 359–402.
Chiou, W.L., Riegelman, S., 1971. Pharmaceutical applications of solid dispersion systems. J. Pharm. Sci. 60, 1281–1302.
Clauss, J., Schmidt-Rohr, K., Spiess, H.W., 1993. Determination of domain sizes in heterogeneous polymers by solid-state NMR. Acta Polym. 44, 1–17.
Colthup, N.B., Daly, L.H., Wiberley, S.E., 1990. Introduction to Infrared and Raman Spectroscopy. Academic Press, Inc., pp. 289–325.
Dvinskikh, S.V., Zimmermann, H., Maliniak, A., Sandstrom, D., 2003. Separated local field spectroscopy of columnar and nematic liquid crystals. J. Magn. Reson. 163, 46–55.
Fox, T.G., 1956. Influence of diluent and copolymer composition on the glass temperature of a polymer system. Bull. Am. Phys. Soc. 1, 123.
Garip, S., Severcan, F., 2010. Determination of simvastatin-induced changes in bone composition and structure by Fourier transform infrared spectroscopy in rat animal model. J. Pharm. Biomed. Anal. 52, 580–588.
Gerber, R., Ryan, J.D., Clark, D.S., 2004. Cell-based screen of HMG-CoA reductase inhibitors and expression regulators using LC–MS. Anal. Biochem. 329, 28–34.
Graeser, K.A., Strachan, C.J., Patterson, J.E., Gordon, K.C., Rades, T., 2008. Physicochemical properties and stability of two differently prepared amorphous forms of simvastatin. Cryst. Growth Des. 8, 128–135.
Hancock, B.C., Shamblin, S.L., Zografi, G., 1995. Molecular mobility of amorphous pharmaceutical solids below their glass-transition temperatures. Pharm. Res. 12, 799–806.
Harper, J.K., Strohmeier, M., Grant, D.M., 2007. Pursuing structure in microcrystalline solids with independent molecules in the unit cell using 1H–13C correlation data. J. Magn. Reson. 189, 20–31.
Hongrapipat, J., Kopeckova, P., Prakongpan, S., Kopecek, J., 2008. Enhanced antitumor activity of combinations of free and HPMA copolymer-bound drugs. Int. J. Pharm. 35, 259–270.
Husak, M., Kratochvil, B., Jegorov, A., Brus, J., Maixner, J., Rohlicek, J., 2010. Simvastatin: structure solution of two new low-temperature phases from synchrotron powder diffraction and ss-NMR. Struct. Chem. 21, 511–518.
Jia, X., Wolak, J., Wang, X.W., White, J.L., 2003. Independent calibration of H-1 spin-diffusion coefficients in amorphous polymers by intramolecular polarization transfer. Macromolecules 36, 712–718.
Johari, G.P., Goldstei, M., 1970. Viscous liquids and glass transition. 2. Secondary relaxations in glasses of rigid molecules. J. Chem. Phys. 53, 2372.
Kothari, K., Ragoonanan, V., Suryanarayanan, R., 2014. Influence of molecular mobility on the physical stability of amorphous pharmaceuticals in the supercooled and glassy states. Mol. Pharm. 11, 3048–3055.
Kopecek, J., Kopeckova, P., Minko, T., Lu, Z.R., Peterson, C.M., 2001. Water soluble polymers in tumor targeted delivery. J. Control. Release 74, 147–158.
Lackowicz, J.R., 2006. Principles of Fluorescence Spectroscopy, third ed. Springer, New York.
Lee, M., Goldburg, W.I., 1965. Nuclear-magnetic-resonance line narrowing by a rotating rf field. Phys. Rev. 140, 1261.
Li, Z.J., Abramov, Y., Bordner, J., Leonard, J., Medek, A., Trask, A.V., 2006. Solid-state acid-base interactions in complexes of heterocyclic bases with dicarboxylic acids: crystallography, hydrogen bond analysis, and N-15 NMR spectroscopy. J. Am. Chem. Soc. 128, 8199–8210.
Lipari, G., Szabo, A., 1982. Model-free approach to the interpretation of nuclear magnetic-resonance relaxation in macromolecules. 1. Theory and range of validity. J. Am. Chem. Soc. 104, 4546–4559.
Nunes, T.G., Viciosa, M.T., Correia, N.T., Danede, F., Nunes, R.G., Diogo, H.P., 2014. A stable amorphous statin: solid-state NMR and dielectric studies on dynamic heterogeneity of simvastatin. Mol. Pharm. 11, 727–737.
Olcak, D., Onufer, J., Mucha, U., Raab, M., Spevacek, J., 2004. Study of motional processes in polymer blends composed of isotactic polypropylene and ethylene-propylene-diene monomer rubber by broad-line H-1 NMR. J. Appl. Polym. Sci. 91, 247–252.
Palmer, A.G., Williams, J., McDermott, A., 1996. Nuclear magnetic resonance studies of biopolymer dynamics. J. Phys. Chem. 100, 13293–13310.
Parhami, F., Beamer, W.G., Tintut, Y., Hahn, T.J., Demer, L.L., 2000. Atherogenic high fat diet lowers bone mineral content and density in mice: possible role of lipid oxidation in osteoporosis. J. Bone Miner. Res. 15, S543.
Paudel, A., Geppi, M., Van den Mooter, G., 2014. Structural and dynamic properties of amorphous solid dispersions: the role of solid-state nuclear magnetic resonance spectroscopy and relaxometry. J. Pharm. Sci. 103, 2635–2662.
Pokharkar, V.B., Mandpe, L.P., Padamwar, M.N., Ambike, A.A., Mahadik, K.R., Paradkar, A., 2006. Development, characterization and stabilization of amorphous form of a low T-g drug. Powder Technol. 167, 20–25.
Policianova, O., Brus, J., Hruby, M., Urbanova, M., Zhigunov, A., Kredatusova, J., Kobera, L., 2014. Structural diversity of solid dispersions of acetylsalicylic acid as seen by solid-state NMR. Mol. Pharm. 11, 516–530.
Rihova, B., Rathi, R.C., Kopecova, P., Kopecek, J., 1992. In vitro bioadhesion of carbohydrate-containing N-(2-hydroxypropyl) methacrylamide copolymers to the GI tract of guinea pigs. Int. J. Pharm. 87, 105–116.
Roper Scientific, Inc. 2000. Etaloning in Back-Illuminated CCDs. Technical Note.
Schmidt-Rohr, K., Clauss, J., Spiess, H.W., 1992. Correlation of structure, mobility, and morphological information in heterogeneous polymer materials by 2-dimensional wideline-separation NMR-spectroscopy. Macromolecules 25, 3273–3277.
Sekiguchi, K., Obi, N., 1961. Studies of absorption of eutectic mixture of sulfathiazole and that of ordinary sulfathiazole in man. Chem. Pharm. Bull. 9, 866–872.

Silva, T.D., Arantes, V.T., Resende, J.A.L.C., Speziali, N.L., de Oliveira, R.B., Vianna-Soares, C.D., 2010. Preparation and characterization of solid dispersion of simvastatin. Drug Dev. Ind. Pharm. 36, 1348–1355.
Simoes, R.G., Bernardes, C.E.S., Diogo, H.P., Agapito, F., Minas da Piedade, M.E., 2013. Energetics and structure of simvastatin. Mol. Pharm. 10, 2713–2722.
Simoes, R.G., Diogo, H.P., Dias, A., Oliveira, M.C., Cordeiro, C., Bernardes, C.E.S., Minas Da Piedade, M.E., 2014. Thermal stability of simvastatin under different atmospheres. J. Pharm. Sci. 103, 241–248.
Song, Y., Wang, L., Yang, P., Wenslow Jr., R.M., Tan, B., Zhang, H., Deng, Z., 2013. Physicochemical characterization of felodipine-kollidon VA64 amorphous solid dispersions prepared by hot-melt extrusion. J. Pharm. Sci. 102, 1915–1923.
Spevacek, J., Brus, J., 1999. Polymer–solvent interactions in thermoreversible gels of isotactic poly(methyl methacrylate) as studied by measurement of H-1 NMR relaxation of the solvent. Macromol. Symp. 138, 117–122.
Tian, B., Zhang, L., Pan, Z., Gou, J., Zhang, Y., Tang, X., 2014. A comparison of the effect of temperature and moisture on the solid dispersions: aging and crystallization. Int. J. Pharm. 475, 385–392.
Ulbrich, K., Subr, V., 2010. Structural and chemical aspects of HPMA copolymers as drug carriers. Adv. Drug Deliv. Rev. 62, 150–166.
Urbanova, M., Brus, J., Sedenkova, I., Policianova, O., Kobera, L., 2013. Characterization of solid polymer dispersions of active pharmaceutical ingredients by F-19 MAS NMR and factor analysis. Spectrochim. Acta A: Mol. Biomol. Spectrosc. 100, 59–66.
Vogt, F.G., Clawson, J.S., Strohmeier, M., Edwards, A.J., Pham, T.N., Watson, S.A., 2009. Solid-state NMR analysis of organic cocrystals and complexes. Cryst. Growth Des. 9, 921–937.
Vogt, F.G., Yin, H., Forcino, R.G., Wu, L., 2013. O-17 solid-state NMR as a sensitive probe of hydrogen bonding in crystalline and amorphous solid forms of diflunisal. Mol. Pharm. 10, 3433–3446.
Williams, M.L., Landel, R.F., Ferry, J.D., 1955. Temperature dependence of relaxation mechanisms in amorphous polymers and other glass-forming liquids. Phys. Rev. 98 1549–1549.
Wu, X.L., Burns, S.T., Zilm, K.W., 1994. Spectral editing in CPMAS NMR – generating subspectra based on proton multiplicities. J. Magn. Reson. Ser. A 111, 29–36.